

Research Paper

Yes-Associated Protein (Yap) Is Necessary for Ciliogenesis and Morphogenesis during Pronephros Development in Zebrafish (*Danio Rerio*)

Liangliang He¹, Wenyan Xu², Ying Jing¹, Ming Wu¹, Shuwei Song¹, Ying Cao²✉, Changlin Mei¹✉

1. Kidney Institute of CPLA, Division of Nephrology, Changzheng Hospital, Second Military Medical University, NO.415 Fengyang Road, Shanghai 200003, China.
2. School of life science and technology, Tongji University, 1239 Siping Road, Shanghai 200092, China

✉ Corresponding authors: yingcao@tongji.edu.cn (Cao Y); chlmei1954@126.com (Mei CL)

© 2015 Ivyspring International Publisher. Reproduction is permitted for personal, noncommercial use, provided that the article is in whole, unmodified, and properly cited. See <http://ivyspring.com/terms> for terms and conditions.

Received: 2014.12.14; Accepted: 2015.04.23; Published: 2015.06.11

Abstract

The Hippo signaling pathway and its transcriptional co-activator Yap are known as essential regulators for cell proliferation and organ size. However, little is known about their roles in kidney development and ciliogenesis. We examined expression of Yap during zebrafish embryogenesis, and its transcripts were detected in pronephric duct, while Yap protein was found to be localized in the cytoplasm and apical membrane in kidney epithelium cells. By morpholino (MO) knockdown of *yap* expression in zebrafish, the injected larve exhibits pronephic cysts and many aspects of ciliopathy, which can be rescued by full-length *yap* mRNA, but not *yap*^{S127A} mRNA. With transgenic *Tg(Na⁺/K⁺ ATPase:EGFP)*, we found that lacking Yap led to expansion and discontinuities of pronephric duct, as well as disorganization of cloaca during pronephros morphogenesis. Mis-located Na⁺/K⁺ ATPase and ciliary abnormalities are also detected in pronephric duct of *yap* morphants. In addition, genetic analysis suggests that *yap* interacts with *ift20*, *ift88* and *arll3b* in pronephric cyst formation. Taken together, our data reveals that Yap is required for pronephric duct integrity, maintenance of baso-lateral cell polarity, and ciliogenesis during zebrafish kidney development.

Key words: Yap; Pronephros; Cyst; Kidney; Cilia; Zebrafish

Introduction

Cilia are microtubule-based organelles extending outward from the basal body and ubiquitously exist in almost all vertebrates. Cilia function in fluid flow generation and integration of environmental cues, playing a critical role in vertebrate physiology and development. Recent years, cilia begin to receive extensive attention since it has been linked to a number of phenotypes, such as hydrocephalus, lateral defects, polycystic liver and kidney disease, retinal degeneration. Mutations in ciliary genes lead to a broad set of developmental and adult human diseases including nephronophthisis, Bardet-Biedl syndrome and Joubert syndrome[1-3]. Genetic and proteome screens have revealed an expanding list of proteins required for generation and maintenance of cilia[4].

Polycystic kidney disease (PKD) is a group of genetic diseases featuring the growth of numerous kidney cysts, which is one of the most common potentially lethal genetic disorders in human[5]. More and more evidences have shown that structural or functional ciliary defects cause PKD. Pathogenic proteins of human autosomal dominant PKD (Polycystin-1 and Polycystin-2) have been detected in renal cilium[6, 7]. The best studied ciliary trafficking protein complexes named intraflagellar transport (IFT) particles, which are organized into distinct A/B complexes, are responsible for retrograde or anterograde transport of the moving cargo between the cell body and the axonemal distal tip respectively. IFT mutant mouse and zebrafish have been reported to develop

kidney cyst[8-13]. Other examples as small GTPase Arl13b, transition zone complexes and BBSome have also showed associations with ciliogenesis and PKD[14-19].

The Hippo pathway is a highly conserved signaling regulating cell growth, differentiation, embryogenesis and tumorigenesis[20-26]. The core pathway in mammalian is that Mst kinase in complex with scaffold protein Sav1, phosphorylates downstream kinase Lats, which in turn phosphorylates transcriptional co-activators Yap and Taz, leading to their cytoplasmic retention. When the Hippo pathway is inactive, dephosphorylated Yap/Taz accumulates in nucleus and promotes transcription of the target genes[27]. Upstream of the core pathway lies a number of cell surface regulators, including cadherins, cell polarity complexes, and GPCRs[28-30].

Previous studies have reported disrupted Hippo pathway in PKD and ciliogenesis. TAZ knockout mice exhibit renal cysts, fewer and shorter cilia in cystic lining epithelia, with down-regulation of ciliary genes as *Kif3a*, *Phkd1*[31-33]. Knockdown of Yap in zebrafish leads to pronephric cyst formation[29]. More recently, Yap nuclear localization is observed in cystic epithelia and dilated tubules of PKD mouse models and patients, suggesting its essential role in progression of PKD[34]. However, the regulating process is barely known.

The zebrafish has emerged as a vertebrate animal model exceptionally suitable for the study of embryogenesis and cyst formation. In this study, we analyzed zebrafish *yap* mRNA expression and protein sublocalization in pronephric duct during embryogenesis. Using antisense morpholino to block the translation of zebrafish Yap, the embryos phenocopy many aspects of ciliopathy and develop pronephric cyst. Detections of these embryos with live, *in vivo* cell imaging, *in situ* hybridization and immunostaining provide evidence that defective pronephros development and cyst formation in *yap* knockdown embryos are correlated with disrupted cell migration, altered basolateral cell polarity and ciliary abnormalities. Further, genetic analysis shows Yap interacts with IFT B complex particles and Joubert syndrome protein Arl13b in cyst formation, suggesting an intricate relationship between Yap and ciliogenesis.

Results

Expression and subcellular localization of Zebrafish Yap in Developing Embryos

During zebrafish embryogenesis, *yap* has been shown as a maternal gene, and the zygotic expression starting from the mid-blastula transition stage was mainly in notochord, eyes, brain, which were almost

cilia related organs[20]. The zebrafish pronephric ducts are also composed of ciliated cells, so we performed *in situ* hybridization (ISH) and observed that *yap* was modestly expressed in the lateral plate mesoderm (LPM) and intermediate mesoderm (IM) from the six-somite stage, and was subsequently appeared in the developing pronephric ducts until at least 3 days post fertilization (d.p.f) (Fig.1A-E), suggesting its potential role in the pronephros development.

Previous study of mammalian YAP demonstrated its dynamical expression during kidney organogenesis[21]. To examine the subcellular Yap distribution in zebrafish pronephro, we implemented whole-mount immunostaining and its expression was detected in the pronephric duct at 24 and 48 hours post fertilization (h.p.f) (Fig.1F-H). The specificity of YAP antibody was demonstrated by western blotting of 1 d.p.f embryos with overexpression of Yap-EGFP or knockdown of endogenous Yap with an antisense MO (Fig.1I). We also injected one-cell zebrafish embryos with plasmid *pTol2-8kb-EGFP-yap* and *Tol2* transposase mRNA to drive fusion protein EGFP-YAP to pronephric duct, and detected a conformity of the subcellular localization of exogenous and endogenous Yap. Magnification view of both anterior and posterior segment of a single pronephric duct revealed that Yap diffusely localized in the cytoplasm ring the nucleus with a concentration near the apical surface. We also double stained the injected embryos with anti-atypical PKC (aPKC) to highlight the apical surface and found that it was co-localized with Yap (Fig.1J-J').

Phenotypic changes after knockdown of zebrafish yap

To determine the role of Yap in zebrafish pronephros development, we used antisense MO against the 5'-UTR to effect a targeted knockdown of Yap. The MO has been previously shown to be efficient for abrogation of gene function in the zebrafish[20] and its effectiveness was confirmed by western blot as well (Fig.1I). Compared with the injection control, *yap* morphants revealed multiple defects from 2.5 d.p.f including pronephric cyst, pericardial edema, hydrocephalus, smaller eyes, a short curved tail, and defective cloaca (Fig.2A-E and Supplementary Fig.S1), which were consistent with *yap* expression pattern shown by ISH. The phenotypes of *yap* morphants were dose dependent and initial experiments were conducted to identify 1.5 pmol as the most effective dose for the MO (Supplementary Fig.S1C and D). Since *yap* morphants showed apoptosis in head during embryogenesis, we co-injected with 0.5 pmol *tP53*MO and excluded the possibility that these phenotypes were nonspecific effects due to up-regulation

of the *p53* apoptosis pathway[35] (Supplementary Fig.S1B and C). More importantly, Yap knockdown induced phenotypes can be rescued with zebrafish full-length *yap* mRNA, demonstrating specificity of the MO. Further, we decided to make clear the functional significant of Yap's activity. The S127 and transcription activation domain is well conserved in zebrafish Yap, which influence the activity form and target genes transcription respectively. We found *yap*^{S127A} mutant mRNA cannot rescue kidney cyst in *yap* morphants while overexpressing Δ TAD Yap

without the transcription activation domain is sufficient to rescue the phenotype (Fig.2I). With Tol2 Kit [36], we also discerned that the fluorescence of mutant S127A Yap was translocated into nucleus with remaining stain near the apical surface (Fig.2F-F'). These results suggest that phosphorylated but not activated Yap played a more important role in zebrafish pronephro development, and maintaining normal subcellular localization may be necessary for Yap's function.

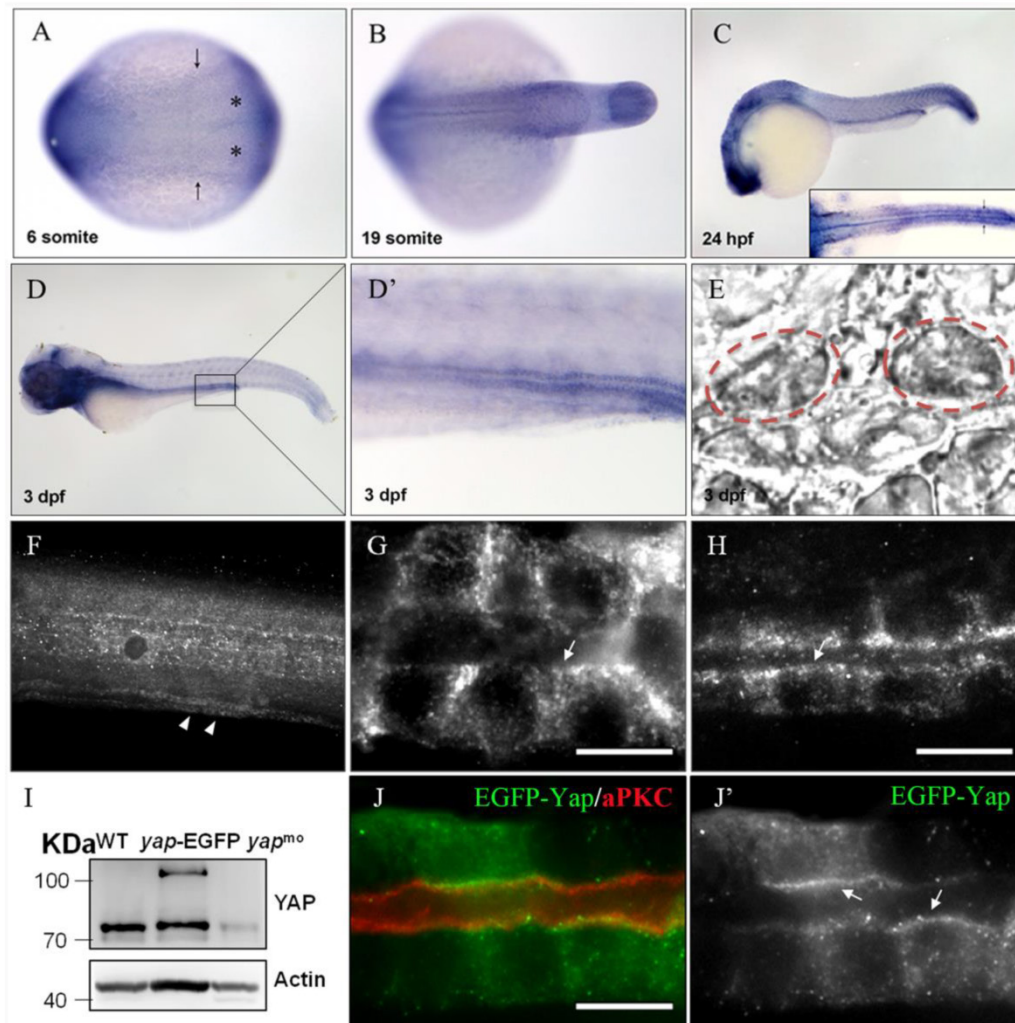


Figure 1. *yap* expression and protein sublocalization during zebrafish nephrogenesis. (A) By whole-mount *in situ* hybridization, *yap* is detected in the LPM (arrows) and IM (asterisk) as early as the 6-somite stage. (B-E) At the 19-somite stage, 24 h.p.f., and 3 d.p.f, *yap* persists in the pronephric ducts, which is confirmed by dorsal view (C; inset), higher magnification view (D') and cross section view (E; dashed red circles). (F) Expression of Yap protein in the trunk of a 2 d.p.f embryo viewed in whole-mount is modest in the pronephric duct (arrowheads). (G-H) A close view of the anterior (G) and posterior (H) segment shows that Yap immunofluorescence is distributed throughout the cytoplasm with a concentration near the apical surface (arrows). (I) Western blot of 1 d.p.f embryos with Yap antibody shows the endogenous Yap at approximately 70 KD, and exogenous Yap-EGFP at 100 KD, while expression of Yap protein in 1 pmol *yap* MO embryos almost disappear. (J-J') With Tol2 kit, exogenous EGFP-Yap distributes in the cytoplasm and has co-localization with the apical marker aPKC (arrows). Bar: 10 μ m.

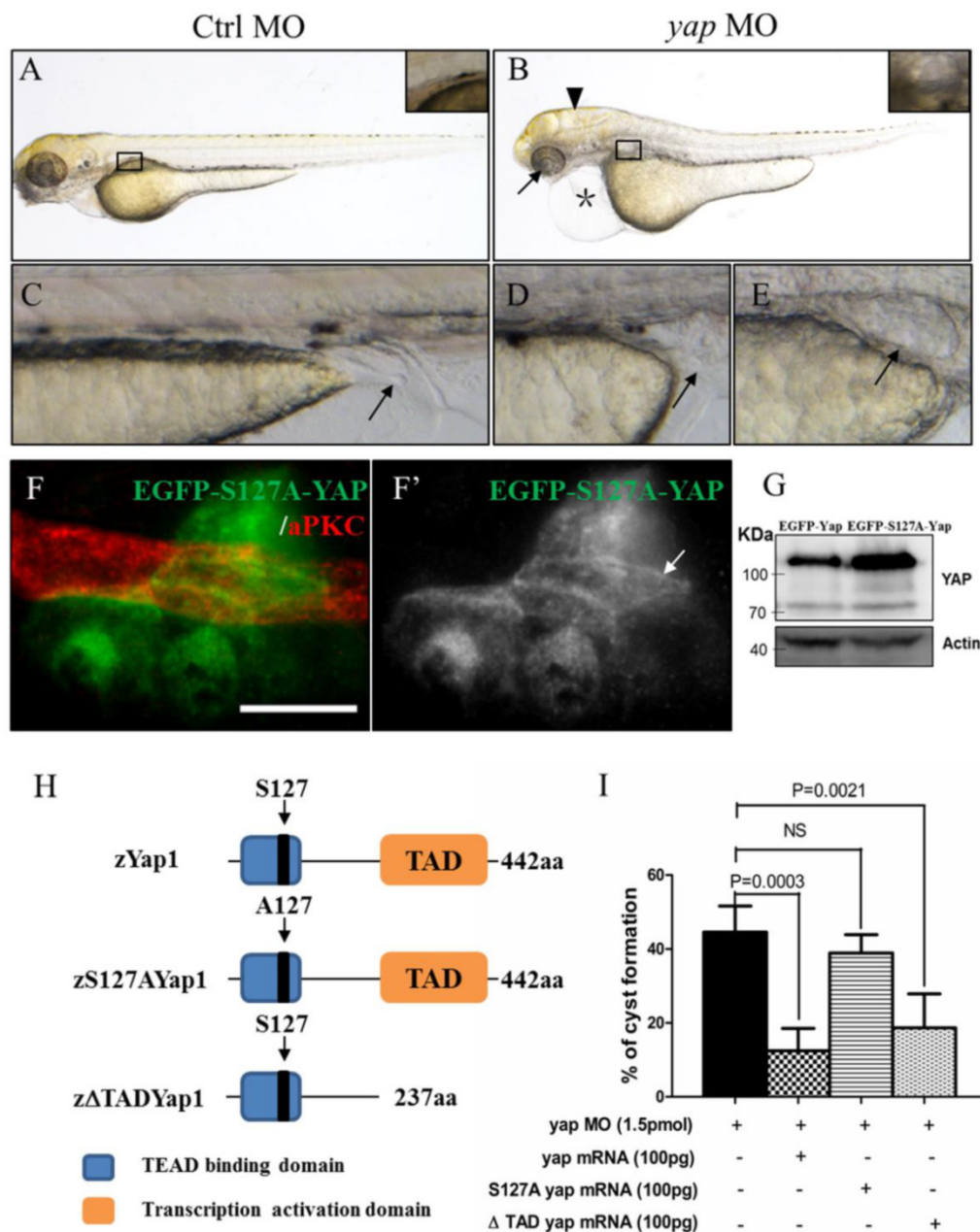


Figure 2. *yap* knockdown by antisense MO results in abnormal phenotypes which can be rescued by full-length and Δ TAD *yap* mRNA. (A-E) Phenotypes of control embryo and *yap* morphant at 3 d.p.f. (B) *yap* morphant exhibit glomerular cyst (inset), heart edema (asterisk), hydrocephalus (arrowhead), smaller eyes (arrow), a short and slightly curved tail. In addition, at the distal end of pronephric duct, the control embryo form obvious outlet at cloaca (C; arrow) while in the morphant, the outlet can't be seen (D; arrow) or is obstructed, promoting dilation or cysts formation (E; arrow). (F-F') Immunostaining shows that exogenous dominant active form EGFP-S127AYap is translocated into nucleus with the apical staining left (F'; arrow). Bar: 10 μ m. (G) Western blot of 2 d.p.f embryos illustrates the protein level of kidney-specifically overexpressed EGFP-Yap and EGFP-S127AYap. (H) Modular structures of zYap1, S127A Yap and Δ TAD Yap. In zYap, the conserved S127 in the TEAD binding domain (aa7-103) is actually located in the aa87. Δ TAD mRNA encodes Yap without the transcription activation domain (aa238-442). aa: amino acids. (I) The pronephric cyst of *yap* MO embryos can be rescued by co-injecting full-length *yap* mRNA and Δ TAD *yap* mRNA ($P < 0.01$), however, co-injecting with *yap*^{S127A} mutant mRNA develops cyst at an average of 38.9%, not significantly different from cyst formation of *yap* morphants with an average of 44.3%.

With *Tg(Na⁺/K⁺ ATPase:EGFP)* fish line, development of pronephric duct is visible, during which the distal tubule cells proliferate and migrate forward, manifesting position and morphology of each nephron segment[37]. We further found loss of integrity of pronephric duct in *yap* morphants. From 1 d.p.f, distal tubular dilation was seen, and disruption of the posterior segment at cloaca existed, including lack of fusion and cyst formation (Fig.3B; arrow). At 2 d.p.f, we

surprisingly found that EGFP labeled pronephric duct was discontinuous (Fig.3D and F; arrowheads), and the ratio increased greatly at 3 d.p.f (Fig.3I), which was mostly detected in the medial tubules. ISH with pronephric duct probe *cadherin (cldh)* 17 in 3 d.p.f morphants verified the same "gap" pattern (Fig.3H). Besides, blocked cell migration was observed during pronephro development (Fig.3J).

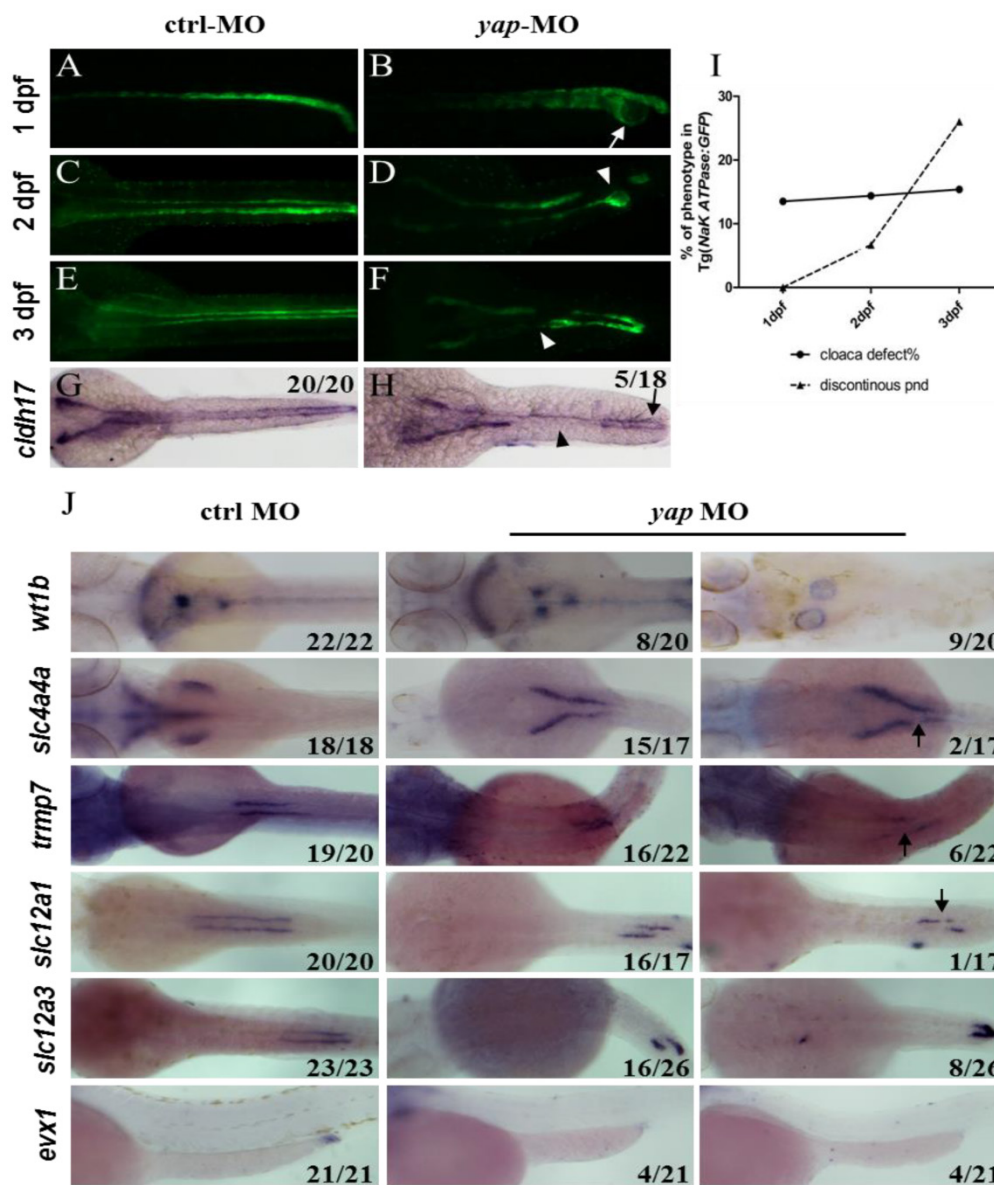


Figure 3. Aberrant morphology of pronephric duct develops during collective cell migration. (A-I) Morphology of pronephric duct labeled by *Tg(Na⁺/K⁺ ATPase:EGFP)* from 1 d.p.f to 3 d.p.f. Disorganization of cloaca occurs in about 15% embryos from 1 d.p.f (B; arrow). Discontinuous pronephric duct is found from 2 d.p.f in 6.7% embryos, and the ratio of occurrence increases sharply to 26% at 3 d.p.f (D and F; arrowheads), *cldhl7* probe shows the similar phenotype (H; arrow and arrowhead). (I) ISH of segment-restricted probe at 3 d.p.f. Pronephric cysts are displayed by *wt1b*. *slc4a4a*⁺ cells fail to migrate towards the glomeruli-neck region compared with the control embryos. Discontinuous segments are found in *slc4a4a*⁺, *trmp-7*⁺, *slc12a1*⁺ cells (arrowheads). Decreased or disappeared expression of *evx1* is seen. The numbers on the lower left of each figure represent the counted phenotypic and total embryos. All photos are dorsal views except for *evx1*, which are lateral views.

PCNA staining showed no change in distal segment cells that excluded the problem with cell proliferation (Supplementary Fig.S3). We next examined a range of segment-restricted markers at 24 h.p.f to assess the pronephro segmentation. The expression pattern of these markers appeared relatively unaffected, demonstrating that the occurrence of defective cloaca and discontinuous pronephric duct was not related with cell fate deficiency (Supplementary Fig.S3). At 3 d.p.f, however, pronephric cysts were displayed by *wt1b* (glomerular marker; Fig.3J). The distribution of epithelium cells in all segments failed to extend towards the head kidney compared with the

control embryos, and proximal segment convolution vanished in *slc4a4a*⁺ cells (PCT segment; Fig.3J). We also found discontinuous expression of *slc4a4a*, *trpm-7* (PST segment), *slc12a1* (DE segment), and decreased or disappeared expression of *evx1* (cloaca maker; Fig.3J). These findings indicate that the defects in pronephric duct develop during collective cell migration and morphogenesis.

Disrupted location of Na⁺/K⁺ ATPase in *yap* morphants

In *yap* morphants, cystic dilation in the glomeruli-neck region were first detected under light micros-

copy at about 50-55 h.p.f. Pronephric cyst is sometimes accompanied by tubular dilation, so we further examined pronephric duct with immunostaining. aPKC indicates the apical membrane as inner diameter of the pronephric duct, and $\alpha 6F$ subunit of Na^+/K^+ ATPase represents basolateral surface as outer diameter. We found tubular dilation develop in both proximal and distal segments of pronephros in 3 d.p.f morphants, and the proximal tubule remained straight with no sign of "hairpin" convolution (Fig.4A-B and S2A). Some studies have reported that altered apico-basal cell polarity in renal epithelia may lead to tubular expansion and cyst formation, e.g. mis-sorting or insertion of transporters and receptors as Na^+/K^+ ATPase, NKCC1 and EGFR[38]. Thus we analyzed Na^+/K^+ ATPase localization in 3 d.p.f embryos with cross section staining. The baso-lateral staining of Na^+/K^+ ATPase was not obvious in a part of enlarged tubules (Fig.4D'; red arrow), and even apical expression was detected (Fig.4D'; arrowhead). Mis-localization of Na^+/K^+ ATPase in renal cells can result in secretion of sodium into the lumen and fluid accumulation[39]. Meanwhile, location of the apical marker, such as aPKC and F-actin, appeared intact (Fig. 4D and S2B). The results suggest that disruption of baso-lateral cell polarity, but not apical polarity, may give rise to cyst formation in *yap* morphants.

Ciliary defects in *yap* morphants

Defects in ciliary genes often lead to pronephric cyst, curved tails, heart edema, smaller eyes in

zebrafish as *yap* morphants exhibit. To examine the effect of Yap in ciliogenesis, we stained the eyes and pronephric ducts of *yap* morphants and control embryos with acetylated α -tubulin. In zebrafish, the outer segment of the photoreceptor is a highly modified cilium giving access to visual transduction, it begins to form by 54 h.p.f and persists thereafter. We found that the outer segments were almost discernable in smaller eyes of 3 d.p.f *yap* morphants (Fig.5A; arrows). The pronephric duct features multiciliated cells (MCCs) and single ciliated cells (SCCs), which form clustered cilia bundles and single cilia respectively. The single cilia are observed as early as 20 h.p.f while the bundling cilia can only be detected from about 36 h.p.f. We examined cilia formation at 3 d.p.f in at least 7 embryos each group, and found that the MCCs in the mid region of the duct did not form normal bundles but only disordered cilia, which had also been seen in other zebrafish cilia mutants [9, 39], while in the posterior segments, the number (20.3 ± 1.5 in morphant versus 30.3 ± 2.7 in wild-type embryos, mean \pm SEM; $P < 0.01$) and length ($3.9 \pm 0.2 \mu\text{m}$ in morphant versus $6.2 \pm 0.2 \mu\text{m}$ in wild-type embryos, mean \pm SEM; $P < 0.001$) of single cilia decreased significantly (Fig.5B-C). More importantly, cilia defects in *yap* morphants could be rescued by overexpression of full-length *yap* mRNA or ΔTAD *yap* mRNA, but not by *yap*^{S127A} mRNA (Supplementary Fig.S4).

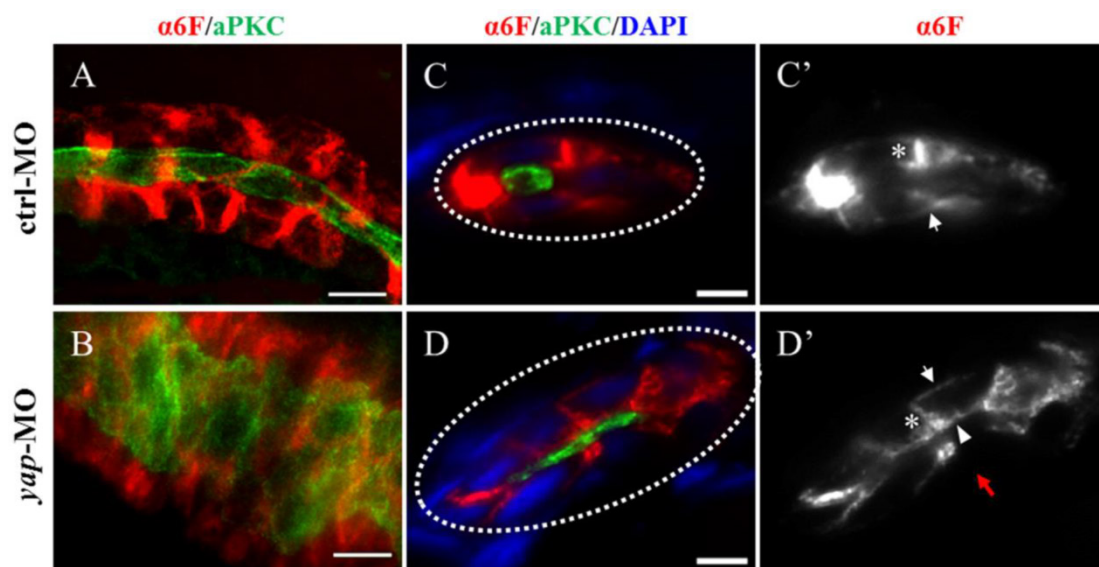


Figure 4. The Na^+/K^+ ATPase is mis-located to the apical surface of pronephric duct in *yap* morphants. (A-B) Whole-mount staining shows that the inner diameter of the enlarged duct indicated by aPKC is about fourfold of the control, however, the change of the outer diameter indicated with α -6F is not that dramatic. (C-D') The cross section view demonstrates increased cell number surrounding the dilated duct compared with the control duct (white dashed circles represent the cross sections of the ducts), the baso-lateral staining of Na^+/K^+ ATPase is not obvious in a part of enlarged tubules (Fig.4D'; red arrow), and even is mis-targeted to the apical surface adjacent to aPKC (D'; arrowhead). (C' and D') Arrows indicate basal surface and asterisks indicate lateral surface. (A-B) Bar: 10 μm . (C-D) Bar: 5 μm .

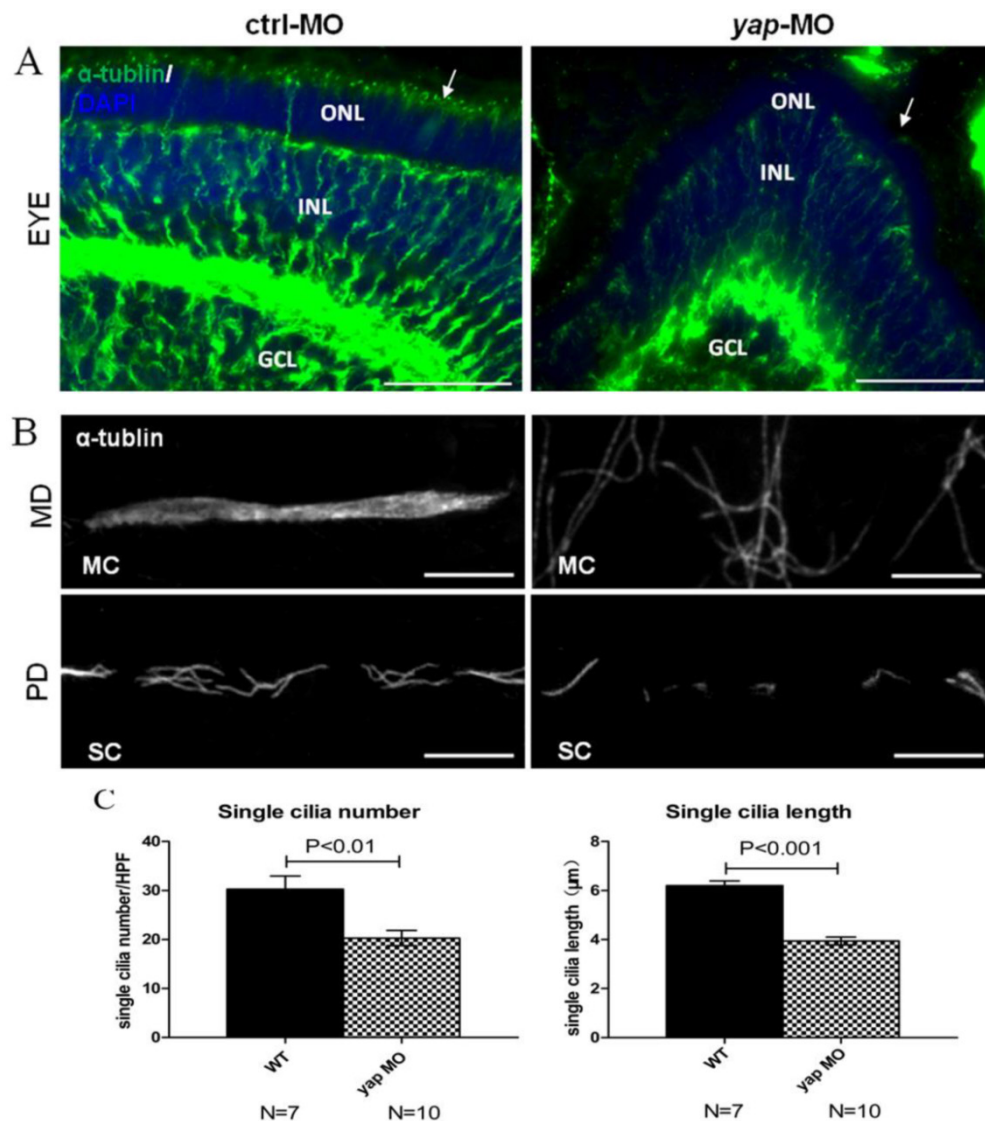


Figure 5. *yap* morphants have ciliary defects. (A) In the eye, the outer segment of photoreceptor cell, which is a modified cilium, is hard to detect in the morphants at 3 d.p.f (the left arrow indicates the control, the right arrow shows defect in *yap* morphant). Bar: 25 μm (B) Compared with the injection control, cilia defects are observed in medial and posterior segment of the pronephric duct in the morphant. Bar: 10 μm. (C) Statistical analysis of the single cilia number per high power field and single cilia length in control and morphant embryos. The cilia are shown by staining with antibody against acetylated α-tubulin. α-tub, anti-acetylated α-tubulin; GCL, ganglion cell layer; INL, inner nuclear layer; ONL, outer nuclear layer; MD, medial segment of pronephric duct; PD, posterior segment of pronephric duct; MC, multicilia; SC, single cilia; HPF, high power field.

Yap influences basal body arrangement and apical membrane docking in ciliogenesis

To further investigate the ciliary defects of *yap* morphants, we performed ISHs for *foxj1a* and *shippo1* (*odf3b*) (Fig.6A). *foxj1a* is a cilia master regulator and one target of Hedgehog signaling, promoting ciliary differentiation and function, and its activity is sufficient for ectopic cilia development[40]. If the ciliary defects in *yap* morphants are *foxj1a* dependent, we would expect decreased level of *foxj1a*. Actually, we found up-regulation of *foxj1a* in both 24 h.p.f and 3 d.p.f *yap* morphants (90% and 70.6% respectively; Fig.6A). We additionally over-expressed *foxj1a* mRNA in wild-type and *yap* morphant embryos to observe its influence in pronephro ciliogenesis. However, little

change had been seen (Supplementary Fig.S4). The results suggest cilia defects in *yap* morphants are *foxj1a* independent, and enhance of *foxj1a* may be a feedback regulation induced by epithelial stretch and cyst formation[41]. *shippo1* is a marker of MCCs[42]. The expression pattern of *shippo1* in 24 h.p.f morphants appeared relatively unaffected (86.7%). But in 3 d.p.f *yap* morphants, *shippo1* labeled MCCs were in a disorganized array and gathered together in the middle region (57.9%), while in control, MCCs placed one by one along the pronephric duct (Fig.6A). Accumulated MCCs could be attributed to defects in lateral inhibition during differentiation of bipotential precursor cells[42] or blocked collective cell migration. Unchanged *shippo1*⁺ and *trpm7*⁺ cells at 24 h.p.f excluded the possibility of biased differentiation to-

wards a MCC fate (Supplementary Fig.S3). Obviously delayed cell migration of *yap* morphants at 3 d.p.f could explain gathered MCCs in the medial segment (Fig.3J).

All cilia are extended from basal bodies which are analogous to mitotic centrioles. In both MCCs and SCCs, ciliogenesis begins with basal bodies apical membrane docking and then acquires accessory structure and elongates[43]. By immunostaining with anti- γ -tubulin and anti-aPKC, we additionally found disordered basal bodies in dilated pronephric duct. In whole-mount staining of 3dpf embryos, basal bodies of a MCC organized in a thread-like array at the apical side in control (Fig.6B'; arrowheads), while in expanded ducts of morphants, the basal bodies of a MCC were accumulated into clusters (Fig.6C'; arrowheads), which had been reported to affect cilia bundling[9]. With cross section staining, failure of basal bodies docking to the apical surface was seen in enlarged pronephric ducts of both anterior and posterior segments, and this might account for cilia defects in SCCs (Fig.6E and G; arrows).

yap* genetically interacts with *ift20*, *ift88* and *arl13b

Given *yap* morphant embryos display shorted cilia length with defective basal body apical docking, we proposed the hypothesis that Yap protein might

participate in ciliary trafficking pathway. The pattern of defective cilia in *yap* morphants is very similar to that of IFT complex B mutants and *arl13b* mutants[9, 15]. IFT complex B is well known for carrying precursors needed for cilia assembly from the synthesis site in the cell body to the assembly site in the cilium. In mouse, IFT20 is the only complex B protein localized to the Golgi apparatus in addition to the cilia and centrosome, and IFT88 is the core protein that assembles other IFT B particles into a complex[44]. Mutation in human *ARL13B* is associated with Joubert syndrome, and it is also responsible for cilia formation and endocytic recycling traffic[15, 45]. Using MO based assay, we first titrated MO against *yap*, *ift20*, *ift88* and *arl13b* to their suboptimal dosages with hardly detectable pronephric cysts (Fig.7A). Then we combined *yap* MO with either of *ift20*, *ift88* and *arl13b* MO to test whether they act synergistically by assessing the percentage of cyst formation. Surprisingly, we found all the three groups of co-injected embryos showed significantly increased percentage of pronephric cysts, and the most marked synergy occurred between *yap* and *arl13b* (Fig.7B-G). This observation suggests that Yap and Arl13b are most likely to participate in overlapping signaling to maintain normal ciliary transport.

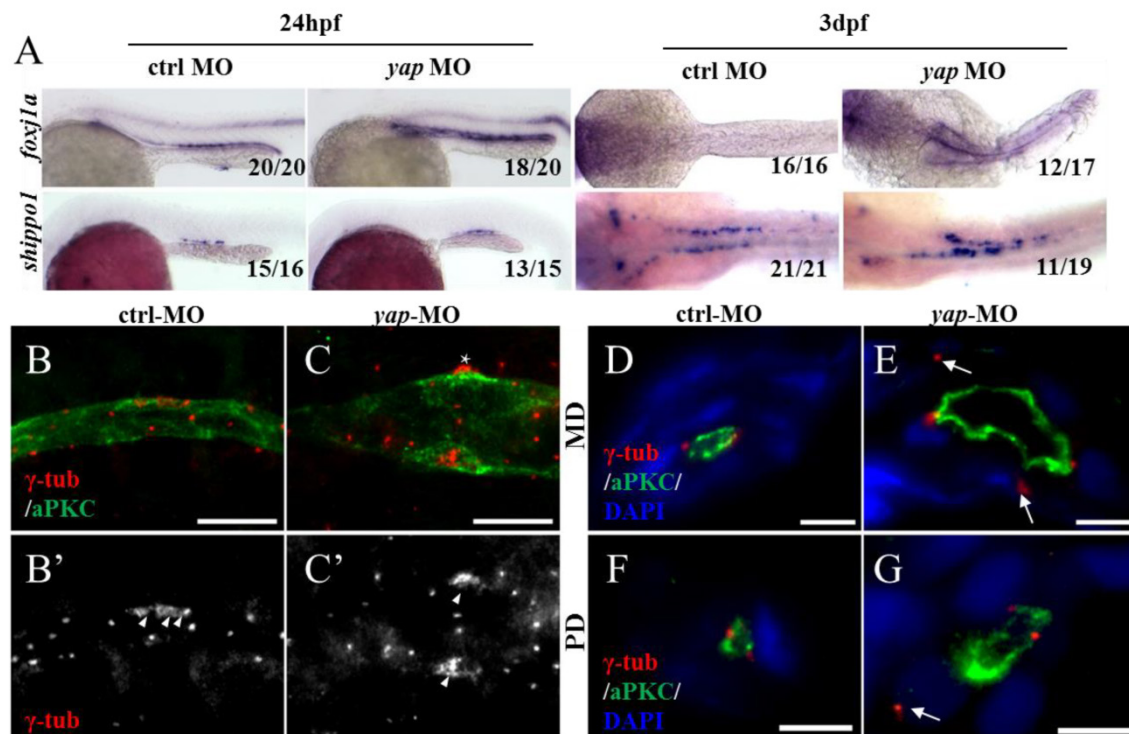


Figure 6. Yap is required for basal body arrangement and apical docking in pronephric duct. (A) The expression level of *foxj1a* (cilia master gene) is increased in 24 h.p.f and 3 d.p.f *yap* morphant. *shippo1* (a marker of MCCs) expression is unaffected in 24 h.p.f *yap* morphant, but is accumulated in the medial pronephric duct in 3 d.p.f morphant. 24 h.p.f embryos are lateral views and 3 d.p.f embryos are dorsal views. (B-C') With anti- γ -tubulin staining, basal bodies of MCCs in 3 d.p.f embryos are showed. In control, basal bodies are in a thread-like array at the apical surface (B'; arrowheads), but in morphant, basal bodies are gathered into clusters (C'; arrowheads) and even out of the edge of apical membrane (C; asterisk). Bar: 10 μ m. (D-G) Cross sections staining show that basal bodies are unable to migrate to the apical surface in enlarged pronephric duct of both proximal and distal segments (E and G; arrows). Bar: 5 μ m. γ -tub, anti- γ -tubulin.

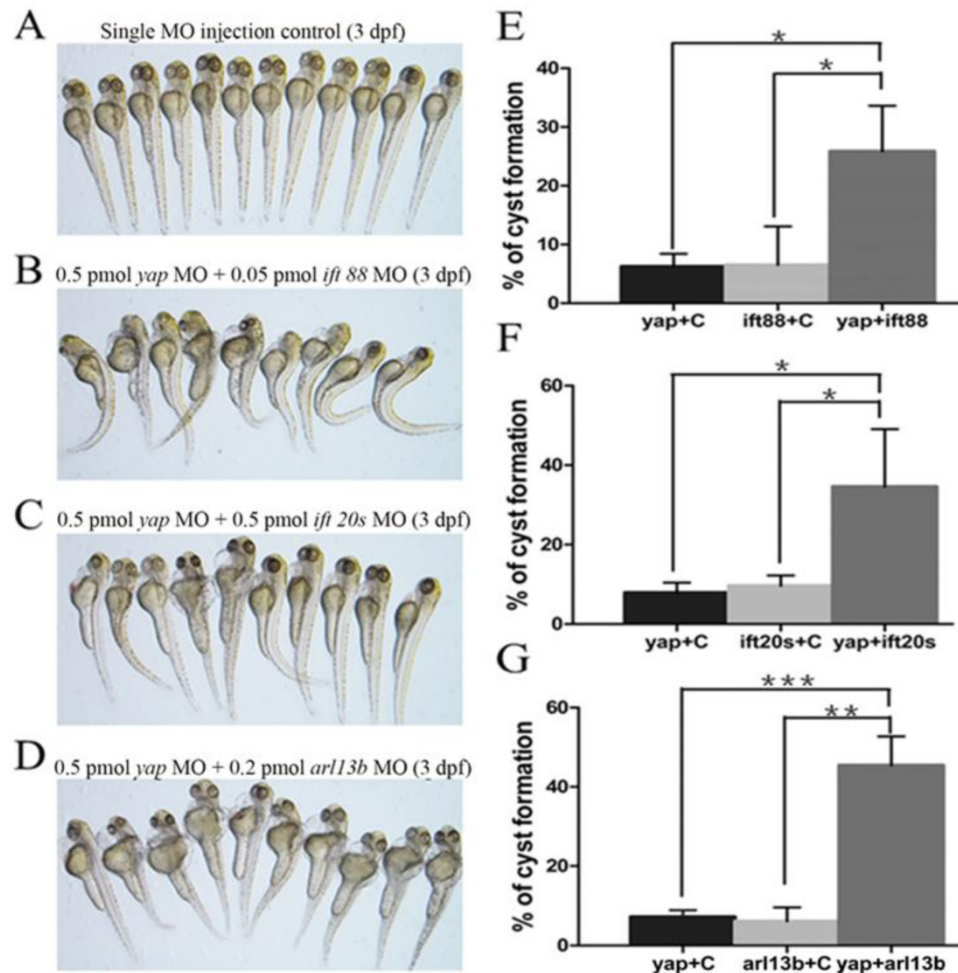


Figure 7. *yap* genetically interacts with *ift20*, *ift88* and *arl13b*. (A-D) Phenotype of embryos injected with suboptimal *yap* MO (0.5 pmol) or/and *ift20s* (0.5 pmol), *ift88* (0.05 pmol), *arl13b* MO (0.2 pmol) at 3 d.p.f. The single MO injection control embryos are almost normal (A) while co-injection embryos exhibit dramatically increased percentage of pronephric cysts, heart edema, tail curvature and smaller eyes (B-D). (E-G) Graphs represent the percentage of embryos that develop pronephric cysts. The single MO injection control is treated with suboptimal single MO and control MO to exclude the effect of mechanical injury to embryos. Each experiment is repeated three times with at least 50 embryos. *: $P < 0.05$; **: $P < 0.01$; ***: $P < 0.001$.

Discussion

The Hippo pathway is a novel signaling and “hot spot” for intensive studies. It is involved in multiple processes such as growth-suppression, cell fate and differentiation, mechanical stress transduction, embryogenesis, and can crosstalk with several important signaling pathways, including Wnt pathway, PCP pathway, Notch Pathway and sonic hedgehog (shh) pathway [20, 24, 29, 46, 47]. Yap is one of transcriptional co-activators of the Hippo pathway, and its relevance to kidney development and PKD has just started to be realized. However, Yap knockout mice is embryonic lethal that limits further study of its *in vivo* function. In this study, we used zebrafish as a model to investigate the role of Yap in kidney development, ciliogenesis and cystogenesis.

The role of Yap in zebrafish pronephros development

Previous study showed that the distribution of Yap is spatially and temporally regulated during mouse kidney development, and knockout of Yap in the cap mesenchymal progenitor cells specifically lead to abnormal nephrogenesis[21]. We found zebrafish Yap is persistently localized in the cytoplasm and apical surface of pronephric duct epithelium cells during embryogenesis, functioning by a non-activated form. Embryos deficient in Yap display discontinuous and dilated pronephric duct, inhibited cell migration as well as defective cloaca, which do not stem from cell fate transition or disruption of cell proliferation, but develop during morphogenesis. The phenotype of pronephric tubule discontinuities and lack of fusion at cloaca is extremely identical to that of *cldh17* MO embryos[48]. In addition, Yap was showed to be linked to Fat-cadherin in flies and zebrafish[29]. The cad-

herin super family is calcium-dependent cell adhesion molecules that play an active role in tissue morphogenesis and patterning. During zebrafish pronephros morphogenesis, pronephric cells have to maintain cell adhesion while migrate collectively[37]. Thus we are in favor of a hypothesis that Yap functions together with cadherin members to affect cell adhesion during morphogenesis of pronephros in zebrafish, and this hypothesis needs to be proved further.

The role of Yap in ciliogenesis

Multiple evidences support an intricate relationship between the cilium and the Hippo pathway. A list of ciliary proteins as NPHP4 and NPHP9 can regulate the activity of the Hippo pathway directly[49, 50]. In kidneys of Taz knockout mice, cystic lining cells carry fewer and shorter cilia with decreased expression of *Tg737*, *Kif3a*, *Dctn5*, which encode proteins involved in cilia structure and function[31]. More recently, *in vitro* study has found that upstream regulator Mst1/2-SAV1 complex establish ciliary assembly and ciliary proteins polarized location in a kinase activity-dependent manner. However, loss of Yap using siRNA does not cause ciliary impairment[51].

We show here that *yap* knockdown in zebrafish with MO assay phenocopies many aspects of ciliopathies, including pronephric cysts, pericardial edema, hydrocephalus, smaller eyes, curved body axis, and these phenotypes are almost in tissues in which *yap* is highly expressed by ISH. The PKD phenotype and cilia defects could be rescued with full-length *yap* mRNA and Δ TAD *yap* mRNA, However, *yap*^{S127A} mRNA does not have the similar rescue effect, suggesting that the role of Yap in ciliogenesis is also in a phosphorylation-dependent manner. We also observe in *yap* MO embryos, the photoreceptor cell cilia, especially the outer segments, are nearly absent, while in pronephric duct, cilia bundling are disrupted with fewer and shorter single cilia. Without the “fluid-pump” effect of cilia bundles, the pronephric fluid flow can't be generated normally, which in turn prevents the cell migration and the proximal segments convolution. We further demonstrated basal bodies defects in organization and apical membrane docking, and ciliary trafficking genes *ift20*, *ift88* *arl13b* genetically interact with *yap* in pronephric cyst formation, suggesting that Yap may participate in multiple ciliary signaling pathways. Together, these results provide a novel insight into the relationship between Yap and ciliogenesis *in vivo* and further our understanding of the Hippo pathway in the cilium.

The role of Yap in PKD

The predominant pathological and physiological

processes of PKD include excessive proliferation and poor differentiation of the renal epithelium cells, as well as alteration of cell polarity and fluid accumulation in cyst. In cystic and dilated tubules of *Pkd1* knockout mouse models, autosomal dominant PKD and autosomal recessive PKD patients, Yap nuclear localization is observed in epithelium cells, suggesting activation of Yap may be a common feature in progression of PKD[34]. A simple interpretation is that activated Yap can promote cell proliferation and cyst formation. In this study, we find that the phosphorylated Yap is necessary for Na⁺/K⁺ ATPase baso-lateral localization and ciliogenesis in renal tubules of zebrafish, uncovering the essential role of non-activated Yap in maintenance of normal kidney morphology. Activity alteration of Yap may accelerate the progression of PKD as well. One hypothesis arising from our data is that activity inhibition of Yap may delay the progression of PKD and provide a novel therapeutic target.

The PCP pathway and Yap in the kidney

Planar cell polarity (PCP) refers to coordinated polarization of cells or cell structures within a plane in relation to the tissue axes, and it is visible in directed cell movement during gastrulating embryos or developing kidney and cilia formation in different organisms[52-55]. In *Drosophila*, the PCP proteins (Fat, Dachous) are major upstream regulators of Hpo signaling activity[56]. In addition, multiple lines of evidences support a close relationship between the PCP pathway and Yap in the kidney: In zebrafish, Yap disinhibition participates in pronephric cyst formation after depletion of Fat1 or Scribble, and *yap* morphants exhibit disrupted dorsoventral expression during gastrulation[25]; In the cystic epithelia of *Pkd1* depletion mouse, strong nuclear Yap accumulation accompanied with up-regulation of PCP component Four-jointed (*Fjx1*) was observed[34]. In this study, defects of basal bodies arrangement and polarized docking were found in Yap knockdown embryos, which are also suggestive phenotypes of PCP abnormalities. Given the associations of the PCP pathway with kidney development, PKD and ciliogenesis, we suggest further studies for the potential crosstalk between non-activated Yap and PCP components in the kidney.

Materials and methods

Zebrafish lines and maintenance

Wild-type zebrafish (Tubigen and TAB strain) and transgenic *Tg(Na⁺/K⁺ ATPase:EGFP)*[42] were raised and maintained as the zebrafish book described [57]. Embryos were kept at 28.5 °C in E3 solution and 0.003% PTU (1-phenyl-2-thiourea, Sigma) was added

to the media at 24 h.p.f to suppress pigmentation.

Plasmid clones

Zebrafish *yap* full length cDNA was cloned by PCR into pCS2 vector and a Gateway entry vector. Zebrafish *yap*^{S127A} cDNA were generated via PCR and subcloning, and this highly conserved phosphorylated site mutation was in the 87th amino acid site in zebrafish actually. mRNA was transcribed using the mMESSAGE mMACHINE SP6 kit (Ambion) as described in the manual after linearization of the constructs with NotI. The *Na*⁺/*K*⁺ *ATPase* promoter was made using an 8kb genomic fragment upstream of the first exon of the *Na*⁺/*K*⁺ *ATPase* locus. Using Gateway cloning Kit [36], constructs of a fluorescence reporter system based on Tol2 transposon were generated, in which EGFP and *yap*/*yap*^{S127A} cDNA were driven by the *Na*⁺/*K*⁺ *ATPase* promoter to especially localize in the pronephric ducts (*pTol2*-8kb-EGFP-Yap/ *pTol2*-8kb-EGFP-S127A).

Whole-mount in situ hybridization

Whole-mount in situ hybridization of zebrafish embryos at 6s, 19 s, 24 h.p.f and 72 h.p.f was performed as described previously [58]. The Probes *yap*, *cldh17*, *nbc1*, *slc20a1a*, *trpM7*, *slc13a1*, *slc12a1*, *slc12a3*, *gata-3*, *evx1*, *shippo1*, *foxj1a* have all been reported [20, 41, 59]. The Digoxigenin-labeled antisense riboprobes were made using the mMESSAGE mMACHINE T7 kit (Ambion).

Frozen section and immunohistochemistry

The embryos were fixed in Dent's fixative (80% methanol:20%DMSO) at -20°C overnight or 4% paraformaldehyde (PFA) in PBST(0.5% Tween20) at room temperature (RT) for 2 hours. For preparation of frozen section, the fixed embryos were gradually dehydrated in 10%, 20%, 30% (w/v) sucrose and embedded in O.C.T in a dry ice bath. Frozen blocks were sectioned at 10 μm thickness with a CM1950 cryotome (Leica). Embryos or section were blocked in 10% normal goat serum and incubated in primary antibody in blocking buffer 2 hours at RT or overnight at 4°C. After washing 3 times with PBST, 1:500 diluted secondary antibodies were used at RT for 2 hours. Washed embryos were finally embedded and photographed on a Nikon eclipse 80i fluorescence microscope.

Microinjection

All MOs (Gene Tools) were diluted with RNA only water and injected into embryos at one-cell stage. The sequences of the MOs were described previously: *yap*5'UTR-MO (5'-CTCTTCTTTCTATCCAACAGAAACC-3'[20]), *tp53*MO (5'-GCGCCATTGCTTTGCAAGAATTG-3'[35]), *ift20SPMO* (5'-CAACAACG

TACCTTCATTTTTTCAG-3'[60]), *ift885*'UTR-MO(5'-CTGGGACAAGATGCACATTCTCCAT-3'[61]), *arl13b*5'UTR-MO (5'-TTTCCCCCCTAAATGCTTTCACCTGG-3'[15]). A standard ctrl MO (5'-CCTCTTACCTCAGTTACAATTTATA-3') was used as a negative control. For rescue experiment, 100pg zebrafish *yap* full-length mRNA or *yap*^{S127A} mRNA was co-injected with *yap*5'UTR-MO into one-two cell stage embryos. *Na*⁺/*K*⁺ *ATPase* promoter constructs in the *pTol2* transposase vector (50 ng/nl) were injected into embryos before one cell stage together with Tol2 transposase mRNA (50 ng/nl) and imaged at later stages.

Western blot analysis

Zebrafish embryo lysates were prepared with 1 d.p.f embryos. To remove the yolk protein, the sample was washed with deolving buffer and washing buffer contain protease inhibitor cocktail (Sigma-Aldrich), and the supernatant was removed following a gentle centrifugation at 300 g for 3 minutes at 4 °C. The embryos were added with 2×SDS loading buffer and homogenized completely, and then boiled for 5 minutes following centrifugation at 14000 g for 10 minutes. Immunoblotting was performed using standard protocols.

Antibodies

The antibodies used in for IF (immunofluorescence) are: mouse anti alpha 6F (*Na*⁺/*K*⁺ *ATPase*) (1:100, Developmental Studies Hybridoma Bank), rabbit anti PKCδ (1:200, Santa Cruz), mouse anti acetylated α-tubulin 6-11b-1 (1:2000, Sigma-Aldrich), mouse anti γ-tubulin (1:100, Sigma-Aldrich), mouse anti GFP (1:500, Roche), rabbit anti YAP (1:50, cell signaling), mouse anti PCNA (1:3000, Sigma-Aldrich), Rabbit antibody to *Cldh17* was raised against two different amino acid peptides (QDVNDNYPKLQKT and CPFTFAISRKSQNFEIKP)(1:300, Biomed). The antibodies used in for Western blotting (WB) are: mouse anti Actin (1:3000, Sigma-Aldrich), rabbit anti YAP (1:200, cell signaling). Secondary antibodies used for IF (Alexa Fluor 488 or 594) and WB (horseradish peroxidase-conjugated) are from Invitrogen and ABGENT, respectively.

Statistical Analysis

Graphpad prism 5.0 was used to derive standard deviation and unpaired Student's *t*-tests.

Supplementary Material

Supplementary Figures S1-S4.

<http://www.ijbs.com/v11p0935s1.pdf>

Abbreviation

Yap: yes kinase-associated protein; MO: morpholino; PKD: polycystic kidney disease; IFT: intraflagellar transport; Arl13b: ADP-ribosylation factor-like 13B; Taz: transcriptional coactivator with PDZ binding motif; GPCRs: G-protein coupled receptors; ISH: *in situ* hybridization; LPM: lateral plate mesoderm; IM: intermediate mesoderm; d.p.f: days post fertilization; h.p.f: hours post fertilization; aPKC: anti-atypical PKC; UTR: untranslated region; MCCs: multiciliated cells; SCCs: single ciliated cells

Acknowledgement

We are grateful for stimulating discussions with members in Cao's lab, Fan Zhang, Miaomiao Jin for providing technical assistance. We would like to thank Dr. Wang Zheng in Prof. Xingzhen Chen's lab for his advice on written English.

Competing Interests

The authors have declared that no competing interest exists.

References

- Sharma N, Berbari NF, Yoder BK. Chapter 13 Ciliary Dysfunction in Developmental Abnormalities and Diseases. In: Bradley KY, editor. *Current Topics in Developmental Biology*. Academic Press; 2008: 371-427.
- Badano JL, Mitsuma N, Beales PL, Katsanis N. The Ciliopathies: An Emerging Class of Human Genetic Disorders. *Annual Review of Genomics and Human Genetics*. 2006; 7: 125-48.
- Davis EE, Katsanis N. The ciliopathies: a transitional model into systems biology of human genetic disease. *Current Opinion in Genetics & Development*. 2012; 22: 290-303.
- Gherman A, Davis EE, Katsanis N. The ciliary proteome database: an integrated community resource for the genetic and functional dissection of cilia. *Nat Genet*. 2006; 38: 961-2.
- Calvet JP, Grantham JJ. The genetics and physiology of polycystic kidney disease. *Semin Nephrol*. 2001; 21: 107-23.
- Pazour GJ, San Agustin JT, Follit JA, Rosenbaum JL, Witman GB. Polycystin-2 localizes to kidney cilia and the ciliary level is elevated in orpk mice with polycystic kidney disease. *Curr Biol*. 2002; 12: R378-80.
- Yoder BK, Hou X, Guay-Woodford LM. The polycystic kidney disease proteins, polycystin-1, polycystin-2, polaris, and cystin, are co-localized in renal cilia. *J Am Soc Nephrol*. 2002; 13: 2508-16.
- Sun Z, Amsterdam A, Pazour GJ, Cole DG, Miller MS, Hopkins N. A genetic screen in zebrafish identifies cilia genes as a principal cause of cystic kidney. *Development*. 2004; 131: 4085-93.
- Cao Y, Park A, Sun Z. Intraflagellar transport proteins are essential for cilia formation and for planar cell polarity. *J Am Soc Nephrol*. 2010; 21: 1326-33.
- Nakanishi K, Sweeney WE, Jr., Avner ED, Murcia NS. Expression of the orpk disease gene during kidney development and maturation. *Pediatr Nephrol*. 2001; 16: 219-26.
- Jonassen JA, SanAgustin J, Baker SP, Pazour GJ. Disruption of IFT complex A causes cystic kidneys without mitotic spindle misorientation. *J Am Soc Nephrol*. 2012; 23: 641-51.
- Davenport JR, Watts AJ, Roper VC, Croyle MJ, van Groen T, Wyss JM, et al. Disruption of intraflagellar transport in adult mice leads to obesity and slow-onset cystic kidney disease. *Curr Biol*. 2007; 17: 1586-94.
- Jonassen JA, San Agustin J, Follit JA, Pazour GJ. Deletion of IFT20 in the mouse kidney causes misorientation of the mitotic spindle and cystic kidney disease. *J Cell Biol*. 2008; 183: 377-84.
- Garcia-Gonzalo FR, Corbit KC, Sirerol-Piquer MS, Ramaswami G, Otto EA, Noriega TR, et al. A transition zone complex regulates mammalian ciliogenesis and ciliary membrane composition. *Nat Genet*. 2011; 43: 776-84.
- Duldulao NA, Lee S, Sun Z. Cilia localization is essential for *in vivo* functions of the Joubert syndrome protein Arl13b/Scorpion. *Development*. 2009; 136: 4033-42.
- Cantagrel V, Silhavy JL, Bielas SL, Swistun D, Marsh SE, Bertrand JY, et al. Mutations in the cilia gene ARL13B lead to the classical form of Joubert syndrome. *Am J Hum Genet*. 2008; 83: 170-9.
- Slanchev K, Putz M, Schmitt A, Kramer-Zucker A, Walz G. Nephrocystin-4 is required for pronephric duct-dependent cloaca formation in zebrafish. *Hum Mol Genet*. 2011; 20: 3119-28.
- Kim YH, Epting D, Slanchev K, Engel C, Walz G, Kramer-Zucker A. A complex of BBS1 and NPHP7 is required for cilia motility in zebrafish. *PLoS One*. 2013; 8: e72549.
- Williams CL, Li C, Kida K, Inglis PN, Mohan S, Semene L, et al. MKS and NPHP modules cooperate to establish basal body/transition zone membrane associations and ciliary gate function during ciliogenesis. *J Cell Biol*. 2011; 192: 1023-41.
- Jiang Q, Liu D, Gong Y, Wang Y, Sun S, Gui Y, et al. yap is required for the development of brain, eyes, and neural crest in zebrafish. *Biochem Biophys Res Commun*; 2009; 389: 114-9.
- Reginensi A, Scott RP, Gregorieff A, Bagherie-Lachidan M, Chung C, Lim DS, et al. Yap- and Cdc42-dependent nephrogenesis and morphogenesis during mouse kidney development. *PLoS Genet*. 2013; 9: e1003380.
- Barron DA, Kagey JD. The role of the Hippo pathway in human disease and tumorigenesis. *Clin Transl Med*. 2014; 3: 25.
- Varelas X. The Hippo pathway effectors TAZ and YAP in development, homeostasis and disease. *Development*. 2014; 141: 1614-26.
- Hao J, Zhang Y, Wang Y, Ye R, Qiu J, Zhao Z, et al. Role of extracellular matrix and YAP/TAZ in cell fate determination. *Cell Signal*. 2014; 26: 186-91.
- Hu J, Sun S, Jiang Q, Sun S, Wang W, Gui Y, et al. Yes-associated protein (yap) is required for early embryonic development in zebrafish (*Danio rerio*). *Int J Biol Sci*. 2013; 9: 267-78.
- Yin M, Zhang L. Hippo signaling: a hub of growth control, tumor suppression and pluripotency maintenance. *J Genet Genomics*. 2011; 38: 471-81.
- Fan R, Kim NG, Gumbiner BM. Regulation of Hippo pathway by mitogenic growth factors via phosphoinositide 3-kinase and phosphoinositide-dependent kinase-1. *Proc Natl Acad Sci U S A*. 2013; 110: 2569-74.
- Genevet A, Tapon N. The Hippo pathway and apico-basal cell polarity. *Biochem J*. 2011; 436: 213-24.
- Skouloudaki K, Puetz M, Simons M, Courbard JR, Boehlke C, Hartleben B, et al. Scribble participates in Hippo signaling and is required for normal zebrafish pronephros development. *Proc Natl Acad Sci U S A*. 2009; 106: 8579-84.
- Curto M, Cole BK, Lallemand D, Liu CH, McClatchey AI. Contact-dependent inhibition of EGFR signaling by Nf2/Merlin. *J Cell Biol*. 2007; 177: 893-903.
- Hossain Z, Ali SM, Ko HL, Xu J, Ng CP, Guo K, et al. Glomerulocystic kidney disease in mice with a targeted inactivation of Wwtr1. *Proc Natl Acad Sci U S A*. 2007; 104: 1631-6.
- Tian Y, Kolb R, Hong JH, Carroll J, Li D, You J, et al. TAZ promotes PC2 degradation through a SCFbeta-Trcp E3 ligase complex. *Mol Cell Biol*. 2007; 27: 6383-95.
- Makita R, Uchijima Y, Nishiyama K, Amano T, Chen Q, Takeuchi T, et al. Multiple renal cysts, urinary concentration defects, and pulmonary emphysematous changes in mice lacking TAZ. *Am J Physiol Renal Physiol*. 2008; 294: F542-53.
- Happe H, van der Wal AM, Leonhard WN, Kunnen SJ, Breuning MH, de Heer E, et al. Altered Hippo signalling in polycystic kidney disease. *J Pathol*. 2011; 224: 133-42.
- Gerety SS, Wilkinson DG. Morpholino artifacts provide pitfalls and reveal a novel role for pro-apoptotic genes in hindbrain boundary development. *Dev Biol*. 2011; 350: 279-89.
- Kwan KM, Fujimoto E, Grabher C, Mangum BD, Hardy ME, Campbell DS, et al. The Tol2kit: a multisite gateway-based construction kit for Tol2 transposon transgenesis constructs. *Dev Dyn*. 2007; 236: 3088-99.
- Vasilyev A, Liu Y, Mudumana S, Mangos S, Lam PY, Majumdar A, et al. Collective cell migration drives morphogenesis of the kidney nephron. *PLoS Biol*. 2009; 7: e9.
- Wilson PD. Apico-basal polarity in polycystic kidney disease epithelia. *Biochim Biophys Acta*. 2011; 1812: 1239-48.
- Sullivan-Brown J, Schottenfeld J, Okabe N, Hostetter CL, Serluca FC, Thiberge SY, et al. Zebrafish mutations affecting cilia motility share similar cystic phenotypes and suggest a mechanism of cyst formation that differs from pkd2 morphants. *Dev Biol*. 2008; 314: 261-75.
- Yu X, Ng CP, Habacher H, Roy S. Foxj1 transcription factors are master regulators of the motile ciliogenic program. *Nat Genet*. 2008; 40: 1445-53.
- Hellman NE, Liu Y, Merkel E, Austin C, Le Corre S, Beier DR, et al. The zebrafish foxj1a transcription factor regulates cilia function in response to injury and epithelial stretch. *Proc Natl Acad Sci U S A*. 2010; 107: 18499-504.
- Liu Y, Pathak N, Kramer-Zucker A, Drummond IA. Notch signaling controls the differentiation of transporting epithelia and multiciliated cells in the zebrafish pronephros. *Development*. 2007; 134: 1111-22.
- Dawe HR FH, Gull K. Centriole basal body morphogenesis and migration during ciliogenesis in animal cells. *J Cell Sci*. 2007; 120: 7-15.
- Follit JA, Xu F, Keady BT, Pazour GJ. Characterization of mouse IFT complex B. *Cell Motil Cytoskeleton*. 2009; 66: 457-68.
- Barral DC, Garg S, Casalou C, Watts GF, Sandoval JL, Ramalho JS, et al. Arl13b regulates endocytic recycling traffic. *Proc Natl Acad Sci U S A*. 2012; 109: 21354-9.
- Tariki M, Dhanyamraju PK, Fendrich V, Borggrete T, Feldmann G, Lauth M. The Yes-associated protein controls the cell density regulation of Hedgehog signaling. *Oncogenesis*. 2014; 3: e112.

- [47]. Dupont S, Morsut L, Aragona M, Enzo E, Giulitti S, Cordenonsi M, et al. Role of YAP/TAZ in mechanotransduction. *Nature*. 2011; 474: 179-83.
- [48]. Horsfield J RA, Reuter K, LaVallie E, Collins-Racie L, Crosier K, Crosier P. Cadherin-17 is required to maintain pronephric duct integrity during zebrafish development. *Mech Dev*. 2002; 115: 15-26.
- [49]. Habbig S, Bartram MP, Muller RU, Schwarz R, Andriopoulos N, Chen S, et al. NPHP4, a cilia-associated protein, negatively regulates the Hippo pathway. *J Cell Biol*. 2011; 193: 633-42.
- [50]. Habbig S, Bartram MP, Sagmuller JG, Griessmann A, Franke M, Muller RU, et al. The ciliopathy disease protein NPHP9 promotes nuclear delivery and activation of the oncogenic transcriptional regulator TAZ. *Hum Mol Genet*. 2012; 21: 5528-38.
- [51]. Kim M, Kim M, Lee MS, Kim CH, Lim DS. The MST1/2-SAV1 complex of the Hippo pathway promotes ciliogenesis. *Nat Commun*. 2014; 5: 5370.
- [52]. McNeill H. Planar cell polarity and the kidney. *J Am Soc Nephrol*. 2009; 20: 2104-11.
- [53]. Romaker D, Puetz M, Teschner S, Donauer J, Geyer M, Gerke P, et al. Increased expression of secreted frizzled-related protein 4 in polycystic kidneys. *J Am Soc Nephrol*. 2009; 20: 48-56.
- [54]. Vervenne HB, Crombez KR, Lambaerts K, Carvalho L, Koppen M, Heisenberg CP, et al. Lpp is involved in Wnt/PCP signaling and acts together with Scrib to mediate convergence and extension movements during zebrafish gastrulation. *Dev Biol*. 2008; 320: 267-77.
- [55]. Cevik S, Sanders AA, Van Wijk E, Boldt K, Clarke L, van Reeuwijk J, et al. Active transport and diffusion barriers restrict Joubert Syndrome-associated ARL13B/ARL-13 to an Inv-like ciliary membrane subdomain. *PLoS Genet*. 2013; 9: e1003977.
- [56]. Reddy BVVG, Irvine KD. The Fat and Warts signaling pathways: new insights into their regulation, mechanism and conservation. *Development*. 2008; 135: 2827-38.
- [57]. Westerfield M. *The Zebrafish Book: A Guide for the Laboratory Use of Zebrafish (Danio rerio)*. Eugene: University of Oregon Press; 2000.
- [58]. Jowett T YY. Double fluorescent in situ hybridization to zebrafish embryos. *Trends Genet* 1996; 12: 387-9.
- [59]. Wingert RA, Selleck R, Yu J, Song HD, Chen Z, Song A, et al. The *cdx* genes and retinoic acid control the positioning and segmentation of the zebrafish pronephros. *PLoS Genet*. 2007; 3: 1922-38.
- [60]. Omori Y, Zhao C, Saras A, Mukhopadhyay S, Kim W, Furukawa T, et al. Elipsa is an early determinant of ciliogenesis that links the IFT particle to membrane-associated small GTPase Rab8. *Nat Cell Biol*. 2008; 10: 437-44.
- [61]. Kramer-Zucker AG, Olale F, Haycraft CJ, Yoder BK, Schier AF, Drummond IA. Cilia-driven fluid flow in the zebrafish pronephros, brain and Kupffer's vesicle is required for normal organogenesis. *Development*. 2005; 132: 1907-21.